

# A New Method of Measuring the Magnetic Field in Hot Plasmas Using Helium Neutral Beam Injection

Yoichi HIRANO, Benjamin HUDSON<sup>1,a)</sup>, Haruhisa KOGUCHI,  
Hajime SAKAKITA and Satoru KIYAMA

*Plasma Frontier Group, National Institute of Advanced Industrial Science and Technology, AIST 1-1-1 Umezono,  
Tsukuba, Ibaraki 305-8568, Japan*

<sup>1)</sup>*Department of Physics, University of Wisconsin, 1150 University Ave., Madison, Wisconsin 53706, USA*

(Received 11 September 2007 / Accepted 5 February 2008)

A new method is proposed to measure the magnetic field direction in hot plasmas using helium (He) neutral beam injection. The injected He beam is ionized by collisions with field electrons, and the ionized He beam atoms emit line radiation during their gyromotion with their rotational axis in the direction of the magnetic field. The direction of that axis can be determined locally from the Doppler width of the line radiation in the region along the beam path. The current intensity and energy of the injected He beam necessary to obtain reasonable intensity of line radiation from He<sup>+</sup> ions are estimated. This estimation includes the effect of ionization from the metastable state of the He beam atoms and takes the 468.6 nm line radiation from He<sup>+</sup> ions as an example. It is shown that the radiation intensity and line broadening width obtained using a He neutral beam with energy of 1 keV and current of 10 mA - 100 mA are sufficient for spectral measurement in typical reversed field pinches. It is also shown that the beam with energy of 10 keV and current of 0.1 - 1 A is sufficient in medium sized tokamaks.

© 2008 The Japan Society of Plasma Science and Nuclear Fusion Research

Keywords: nuclear fusion, magnetic confinement, magnetic field measurement, helium beam injection, helium ions gyromotion, Doppler broadening

DOI: 10.1585/pfr.3.015

## 1. Introduction

There are several methods of measuring the magnetic field in plasma. The most convenient and traditional method is to use a magnetic pick-up coil probe, which is inserted into the plasma and detects the variation in the magnetic field inductively. The magnetic probe is widely used in the measurement of low temperature plasma, but its use in hot plasma is limited because of damage to the probe itself and contamination of the plasma by probe materials. Therefore, the probe cannot be used in the hot, dense plasma usually realized in magnetic confinement experiments for nuclear fusion research.

Instead, a measurement method based on the motional Stark effect (MSE) is widely used in confinement systems of high temperature plasma with a strong magnetic field, such as tokamaks and helical devices [1]. However, a high power density neutral beam injection in a strong magnetic field is preferred for MSE measurement, and hence this method is not easy in a confinement system with a weak magnetic field, such as a reversed field pinch (RFP) and a spherical tokamak. In spite of these difficulties, the MSE was applied to a RFP experiment in Madison Symmetric Torus (MST), and the value of the magnetic field at the plasma center (as low as 0.2 T) was successfully measured [2].

Faraday rotation of a polarized laser beam is also used to measure the magnetic field parallel to the beam [3]. The profile and fluctuation of the magnetic field in MST have been measured successfully by this method [4]. Faraday rotation, however, is the combined integral effect of the density and the magnetic field direction along the laser beam path through the plasma. Therefore, the density profile should be known precisely for estimating the magnetic field profile, which complicates the analysis.

Here, a new method is proposed to measure the magnetic field in hot plasma, by which the local direction of the magnetic field can be obtained. A schematic drawing of the measurement system is shown in Fig. 1, where a helium (He) neutral beam is injected perpendicular to the magnetic field into hot plasma, probably on the equatorial plane of the machine (up and down symmetry may be assumed). Injected He beam atoms are ionized to He<sup>+</sup> by collision with electrons in the plasma. After the ionization, the He<sup>+</sup> ions exhibit the gyromotion in the magnetic field and emit line radiation during their gyromotion until the He<sup>+</sup> ions are fully ionized or leave from the detection region by various drift motions.

By measuring the line radiation from He<sup>+</sup> ions, an inclination of the axis of the gyromotion (hence the direction of the magnetic field) can be determined from the Doppler width of that radiation, since the rotational axis of gyromotion is in the direction of the magnetic field, and the

author's e-mail: y.hirano@aist.go.jp

<sup>a)</sup> Present affiliation; Lawrence Livermore National Laboratory

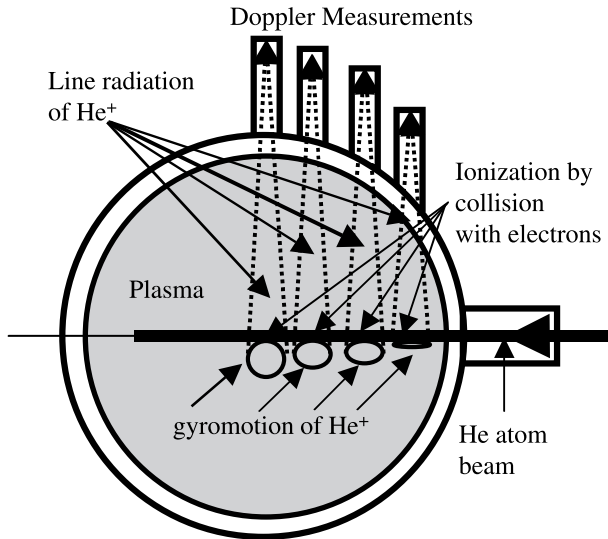


Fig. 1 Schematic diagram of the measurement system. Only a few representative orbits of gyromotion are shown.

speed of the motion, which is the initial beam speed, is monochromatic. Detector positions are selected to optimize the spectral resolution for the inclined angle of the axis of gyromotion. The spatial distribution of the direction of the magnetic field lines can be obtained by measuring the angles at multiple points along the beam line. Two or more detectors in different positions for a certain detection region can be used to improve the angle resolution.

The beam should be injected perpendicular to the magnetic field as precisely as possible, since the component of the beam velocity parallel to the magnetic field can cause drift along the magnetic field line, and the He<sup>+</sup> ions leave rapidly from the detection region if the parallel velocity component is significant.

To examine the feasibility of this method, the following parameters should be considered. Estimation of them will give the intensity and energy of the injected He beam required to obtain reasonable radiation intensity in the Doppler broadening measurement of a selected line, e.g., the well-known 468.6 nm line radiation of He<sup>+</sup> ion.

1. Penetration length of the beam ( $d_D$ ), which depends on the injected beam energy ( $E_b$ ), plasma density ( $n$ ), and temperature ( $T$ ).
2. Value of the gyroradius of He<sup>+</sup> ions ( $r_L$ ) in the magnetic field, which determines the spatial resolution and depends on the beam energy and magnetic field strength ( $B$ ).
3. Life time of He<sup>+</sup> ions ( $\tau_{ion2}$ ) until being fully ionized or lost by charge exchange, which is also determined by the plasma density and temperature.
4. Loss time ( $\tau_{loss}$ ) during which the He<sup>+</sup> ions stay in the detection region ( $V_{obs}$ ). This is determined by the speed of various drift motions.

5. Strength of line radiation ( $I_{4686}$ ) to obtain sufficient photon counts ( $N_{count}$ ).
6. Required wavelength resolution in the Doppler width measurement.

In this study, the above parameters are evaluated for plasma with reasonable density and temperature profiles. In the following study, we consider pure hydrogen (H) plasma and assume that electrons and ions have the same  $T$  and  $n$  values.

First, basic considerations for estimating the above parameters are described, several of which are estimated approximately with homogeneous plasma temperature and density profiles. After that, detailed evaluations are performed by considering the radial variations of He beam penetration and line radiation from He<sup>+</sup> ions, assuming realistic profiles of temperature, density, and magnetic and electric fields for a typical reversed field pinch (RFP) plasma. The effect of the metastable state of He atoms is also taken into account. It is shown that magnetic field direction measurement is feasible if a He neutral beam with relatively low energy (1-10 keV) and current in the range of 0.01-1 A can be injected into the plasma.

## 2. Basic Considerations for the Feasibility of Measurement

### 2.1 Penetration of a helium neutral beam through hot, dense plasma

The penetration of the He neutral beam is one of the most serious considerations for the feasibility of this measurement. Since the effects of slowing down and diffraction of the He neutral beam by collision with hydrogen ions are small in the low energy range considered here [5], the penetration length ( $d_D$ ) of the injected beam is mainly determined from the characteristic lengths of ionization by plasma electrons ( $d_{ion1}$ ) and charge exchange with plasma ions ( $d_{ex1}$ ). This is given by the following equation.

$$d_D = d_{ion1}d_{ex1}/(d_{ion1} + d_{ex1}), \quad (1)$$

where  $d_{ion1} = v_b/(nS_{ion1G})$  and  $d_{ex1} = 1/(n\sigma_{ex1})$ .  $S_{ion1G}$  is the ionization rate coefficient for ionization of He atoms at ground level to He<sup>+</sup> ions by electron impact,  $v_b$  is the beam velocity, and  $\sigma_{ex1}$  is the charge exchange cross-section of He atoms with hydrogen ions (H<sup>+</sup>) [6]. Here, the value of  $S_{ion1G}$  is calculated using the equation for the ionization cross-section given in Ref. [7]. When the electron temperature is in the range of 0.2 - 1 keV,  $S_{ion1G}$  is nearly constant, e.g.,  $S_{ion1G}$  is  $4.5 \times 10^{-14}$  m<sup>3</sup>/s at  $T = 0.5$  keV.

At this stage, ionization from the metastable excited state of He atoms is not taken into account. The effect of the metastable state is considered in Chapter 3 and discussed in Sec. 4.2. The effect of ionization by H<sup>+</sup> impact is also neglected here. It is slightly significant in the case of a tokamak with large  $E_b$ , which is considered in Chapters 3 and 4.

The detailed estimation of the penetration of the He atom beam in the hot, dense plasma is given in Ref. [8] for beam energies higher than 25 keV, where ionization from excited states, by proton collision and by impurities is taken into account. It is shown that ionization from excited states is important if the product of the density and the penetration length ( $nd_D$ ) is greater than  $10^{20} \text{ m}^{-2}$ . In the situation considered here,  $nd_D$  is in the range of  $10^{19} \text{ m}^{-2}$  and the beam energy is less than 10 keV. Therefore, the effects of excited states and proton collision can be neglected excluding the effect of the metastable state.

The effect of ionization by electron impact is dominant in the decay of a neutral beam with  $E_b$  less than 20 keV, and charge exchange becomes significant for  $E_b$  greater than 20 keV. The effect of charge exchange is the most significant at  $E_b \sim 80 \text{ keV}$ . As shown in the next section, the spatial resolution requires a low energy beam, consequently, ionization has the largest effect on the decay of the beam.

Using  $n = 2 \times 10^{19} \text{ m}^{-3}$ ,  $T = 0.5 \text{ keV}$  and  $E_b = 1 \text{ keV}$ , which correspond approximately to the values in the large RFP machines such as Toroidal Pinch Experiment-RX (TPE-RX) [9], Reversed Field pinch Experiment (RFX) [10], and MST [11], and assuming flat profiles of  $n$  and  $T$ ,  $d_{\text{ion1}}$  is 0.24 m,  $d_{\text{ex1}}$  is 290 m ( $\sigma_{\text{ex1}} = 1.7 \times 10^{-22} \text{ m}^{-2}$ ),  $d_D$  is 0.24 m, and nearly 12.5% of the injected beam can penetrate into the plasma with a penetration length of 0.5 m. With these values, the measurement proposed here is feasible.

## 2.2 Minimum limit for the magnetic field strength

In this measurement, the spatial resolution is primarily determined by the gyroradius of the  $\text{He}^+$  ion. For example, to obtain a resolution of  $2r_L = 5 \text{ cm}$ ,  $E_b$  should be less than 1 keV for  $B = 0.37 \text{ T}$ . Since  $r_L$  is proportional to  $E_b^{0.5}$ , lower energy is preferable for better spatial resolution. However, for  $E_b$  less than 1 keV, it is difficult to obtain a beam with sufficient current density. If a spatial resolution of 10 cm is tolerable, then  $B \sim 0.2 \text{ T}$  will be feasible with  $E_b = 1 \text{ keV}$ . Therefore, the feasibility of measuring weak magnetic field with strength less than 0.2 T is fully dependent on future improvement in the low energy beam technology.

## 2.3 Number of $\text{He}^+$ ions in the detection region

The number of  $\text{He}^+$  ions in the detection region is estimated by considering the balance between the production and loss of  $\text{He}^+$  ions in this region.

$\text{He}^+$  ions in this region are produced by ionization of the He neutral beam atoms. The loss of  $\text{He}^+$  ions is caused by further ionization to  $\text{He}^{2+}$  ions by electron impact or charge exchange with hydrogen ions, by neutralization through charge exchange with the remaining hydrogen

atoms in the plasma, and through various drift motions by which the  $\text{He}^+$  ions leave from the detection region.

Considering the short time during which the  $\text{He}^+$  ions stay in the detection region, typically less than  $5 \mu\text{s}$  as shown in later, the effect of the slowing down and diffraction of  $\text{He}^+$  ions by collision with hydrogen ions can also be neglected for energy in the considered range [5]. Therefore, in the steady state, the number of  $\text{He}^+$  ions ( $N_{\text{He}^+}$ ) in the detection region with volume  $V_{\text{obs}}$  is given by the following equation,

$$N_{\text{He}^+}(1/\tau_{\text{loss}} + 1/\tau_{\text{ion2}}) = C_{\text{ion1}} + C_{\text{ex1}}, \quad (2)$$

where  $N_{\text{He}^+} = n_{\text{He}^+}V_{\text{obs}}$  ( $n_{\text{He}^+}$  is the  $\text{He}^+$  ion density),  $\tau_{\text{loss}}$  is the escape time of the  $\text{He}^+$  ions from the detection region by drift motions, and  $\tau_{\text{ion2}}$  is the ionization time for ionization from  $\text{He}^+$  to  $\text{He}^{2+}$  given by  $\tau_{\text{ion2}} = 1/(nS_{\text{ion2}})$ , where  $S_{\text{ion2}}$  is the ionization rate coefficient for ionization from  $\text{He}^+$  to  $\text{He}^{2+}$  by electron impact. The temperature dependence of  $S_{\text{ion2}}$  is calculated using the value given in Ref. [12], (e.g.,  $S_{\text{ion2}} = 3.7 \times 10^{-15} \text{ m}^3/\text{s}$  at  $T = 0.5 \text{ keV}$ ). The charge exchanges from  $\text{He}^+ + \text{H}^+$  to  $\text{He}^{2+} + \text{H}$ , and from  $\text{He}^+ + \text{H}$  to  $\text{He} + \text{H}^+$  are neglected, since their effects are much smaller than that of electron impact in the considered beam energy region ( $E_b < 10 \text{ keV}$ ) [13].

$C_{\text{ion1}}$  is the source term of the  $\text{He}^+$  ions produced by ionization from He beam atoms by electron impact and  $C_{\text{ex1}}$  is that by charge exchange with hydrogen ions. They are given by

$$C_{\text{ion1}} = nn_b S_{\text{ion1G}} A_b \delta l, \quad (3)$$

$$C_{\text{ex1}} = nn_b v_b \sigma_{\text{ex1}} A_b \delta l, \quad (4)$$

where  $n_b$  is the He neutral beam density at the ionization point,  $A_b$  is the beam cross-section and  $\delta l$  is the length of He beam line within the detection region.

$\tau_{\text{loss}}$  is approximately given by

$$\tau_{\text{loss}} = \delta L / v_d \quad (5)$$

where  $\delta L$  is the characteristic length of the detection region,  $V_{\text{obs}} \sim (\delta L)^3$ , and  $v_d$  is the speed of drift motion of the  $\text{He}^+$  ion. Hereafter, we will use  $\delta L = 0.1 \text{ m}$  and assume that  $\delta l = \delta L$ .

Since the difference in  $\text{He}^+$  densities will be small at both ends of the detection region boundary along the beam line, the effect of  $\text{He}^+$  ion flow in and out along the beam line can be neglected. Therefore, it is necessary to consider the motion of  $\text{He}^+$  ions in the direction across the beam line for estimating the loss of  $\text{He}^+$  ions from the detection region. Here three kinds of drift motions, gradient  $B$  drift,  $E \times B$  drift, and parallel drift, are taken into account.

Strictly speaking, the escape time should be estimated by considering the actual gyromotions of the  $\text{He}^+$  ions in the given magnetic field, since their gyroradii cannot be neglected compared with the size of the detection region. However, these estimations require a detailed design of the assembly of the detection system, and such a detailed de-

sign is not necessary for the present estimation of the feasibility of this diagnostic method.

## 2.4 Estimation of intensity of 468.6 nm line radiation

The total intensity of the line radiation [photons/s] from the He<sup>+</sup> ions in the detection region is given by,

$$I_{4686} = nX_{\text{rad}}N_{\text{He}^+}, \quad (6)$$

where  $X_{\text{rad}}$  is the radiation rate coefficient corresponding to the observed line.

Considering the visible 468.6 nm line radiation of the He<sup>+</sup> ions, which corresponds to the transition from the  $n = 4$  level to the  $n = 3$  level, and assuming almost all the ions are in the ground ( $n = 1$ ) state (Corona Model), we estimate the value of  $X_{\text{rad}}$ . In the estimation, the excitations from the ground state to  $4S$ ,  $4P$ ,  $4D$  and  $4F$  levels are considered individually, and the radiative transitions from those four levels to the  $n = 3$  levels are summarized by taking into account the branching ratios from the  $4S$ ,  $4P$ ,  $4D$  and  $4F$  levels to all permitted lower levels. Individual rate coefficients for excitation from the ground state to the  $4S$ ,  $4P$ ,  $4D$  and  $4F$  levels are calculated from the excitation cross-sections given in Ref. [14], and the individual radiative de-excitation rate coefficients are estimated using the branching ratios deduced from the transition probabilities listed in Ref. [15]. The value of  $X_{\text{rad}}$  is  $1.2 \times 10^{-17}$  m<sup>3</sup>/s at  $T = 0.5$  keV. The excitations from the metastable state and other excited states, and de-excitation to the  $n = 4$  levels from higher levels are not taken into account. These effects will enhance the radiation of the 468.6 nm line and the present  $X_{\text{rad}}$  will give a low estimation.

## 3. Estimation of Intensity of 468.6 nm Line Radiation in a RFP Configuration

Here we examine the feasibility of this measurement method in a realistic RFP configuration. We calculate the radial variations of the He beam density, He<sup>+</sup> density, and intensity of He<sup>+</sup> 468.6 nm line radiation in a RFP plasma similar to the MST, which has the major/minor radii ( $R/a$ ) of 1.5 m / 0.52 m [11]. In this calculation we include the effect of the metastable state of He neutral atoms, which significantly affects the ionization from He to He<sup>+</sup> if the initial ratio ( $\gamma_{\text{meta}}$ ) of the density of He atoms in metastable state to the total He atom density is large at the injection point of the beam, since the ionization coefficient for ionization from the metastable state is much larger, by almost an order of magnitude, than that from the ground state. The effect of variation of  $\gamma_{\text{meta}}$  will be estimated in the next chapter.

Assuming the steady state and taking the beam line as the  $x$ -axis ( $x = 0$  is the plasma center and the beam is injected at  $x = a$ ), the equations for He beam density

variation become

$$-v_b(dn_{\text{HeG}}/dx) = -nn_{\text{HeG}}S_{\text{ion1G}} - nn_{\text{HeG}}X_{\text{GM}} - nn_{\text{HeG}}\sigma_{\text{ex1}}v_b - nn_{\text{HeG}}\sigma_{\text{ion1}}v_b, \quad (7)$$

$$-v_b(dn_{\text{HeM}}/dx) = -nn_{\text{HeM}}S_{\text{ion1M}} + nn_{\text{HeG}}X_{\text{GM}} - nn_{\text{HeM}}\sigma_{\text{ex1}}v_b - nn_{\text{HeM}}\sigma_{\text{ion1}}v_b, \quad (8)$$

where  $n_{\text{HeG}}$  is the He beam density at the ground state,  $n_{\text{HeM}}$  is that at the metastable state,  $S_{\text{ion1M}}$  is the electron impact ionization rate coefficient for ionization from metastable state,  $X_{\text{GM}}$  is the excitation coefficient for excitation from the ground state to metastable state,  $\sigma_{\text{ion1}}$  is the cross-section for ionization with H<sup>+</sup> ion impact. The temperature dependences of  $S_{\text{ion1G}}$ ,  $S_{\text{ion1M}}$ , and  $X_{\text{GM}}$  are calculated using the estimation formulas for the corresponding ionization cross-section given in Ref. [7]. The ion impact ionization cross-section is not significant in the low beam energy region with energies less than  $E_b = 10$  keV as shown in Ref. [16]. For example, the value of  $\sigma_{\text{ion1}} v_b$  is  $2 \times 10^{-16}$  m<sup>3</sup>/s for  $E_b = 1$  keV, which is smaller than  $S_{\text{ion1G}}$  by two orders of magnitude.

When including the effect of the metastable state, the source term for the He<sup>+</sup> ions in Eq. (2) is modified to

$$C_{\text{ion1}} + C_{\text{ex1}} = [nn_{\text{HeG}}S_{\text{ion1G}} + nn_{\text{HeM}}S_{\text{ion1M}} + n\sigma_{\text{ex1}}v_b(n_{\text{HeG}} + n_{\text{HeM}})]A_b\delta l, \quad (9)$$

We assume radial profiles of  $[1 - (r/a)^4]$  for both density and temperature with values of central plasma density,  $n_c = 2 \times 10^{19}$  m<sup>-3</sup>, edge plasma density,  $n_w = 1 \times 10^{18}$  m<sup>-3</sup>, central temperature,  $T_c = 500$  eV, and edge temperature  $T_w = 10$  eV, which are not too different from the experimental values obtained in MST. We use the values of  $E_b = 1$  keV, beam radius  $r_b = 1.5$  cm, and injected beam current  $I_{b0} = 100$  mA. The initial value of beam density is given by  $n_{b0} = I_{b0}/(\pi e v_b r_b^2)$ , ( $e$  is the elementary charge). Because a large beam current is difficult to obtain in the low beam energy region, this small value of  $I_{b0}$  is used in the estimation. Recent development of He ion beam source technology suggests that this level of beam current will be feasible with a reasonable injector size [17, 18].

We also use the magnetic field profiles estimated from the experimental MST results, whose radial profiles are shown in Fig. 2, where the poloidal field at the plasma edge ( $B_{\text{pa}}$ ) is set to be 0.3 T. This value corresponds to a plasma current of 780 kA, which is slightly larger than the value achieved experimentally so far in the MST. As shown in Fig. 2, the magnetic field strength is 0.8 T at the plasma center ( $B_{\text{c}}$ ) and 0.3 T at the edge ( $B_{\text{pa}}$ ).  $r_L$  is  $\sim 3$  cm for  $E_b = 1$  keV near the edge, which can provide a reasonable spatial resolution.

An assumed profile of the radial electric field ( $E_r$ ) is also shown in Fig. 2, whose value at the edge ( $E_{\text{rw}}$ ) is 5 kV/m, which is probably higher than the experimental value. The radial profile of  $E_r$  is assumed to be given by  $E_r = E_{\text{rw}}(r/a)^2[2 - (r/a)^2]$ .

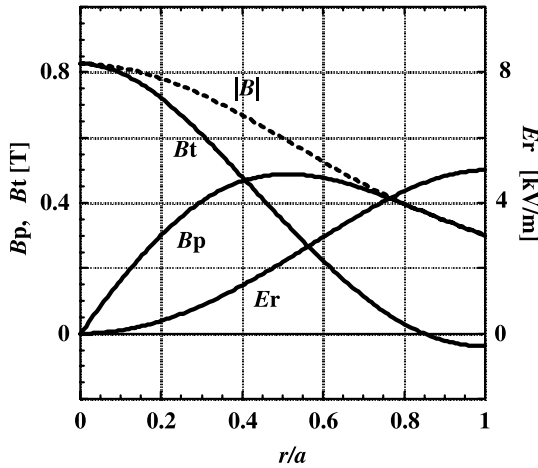


Fig. 2 Radial profiles of the magnetic and electric fields used in the estimation. Suffixes r, p, and t indicate the radial, poloidal, and toroidal components, respectively.

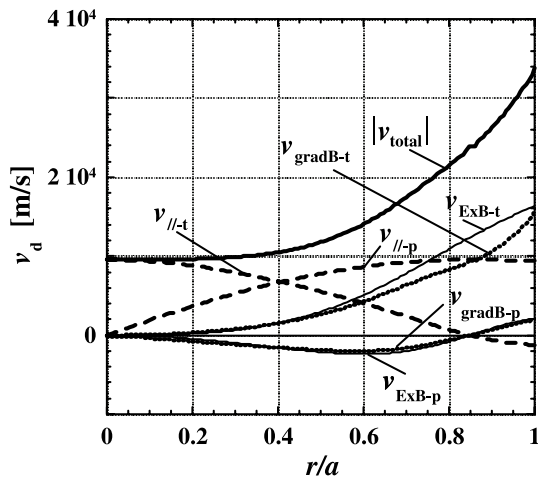


Fig. 3 Radial profiles of various drift motions that mainly contribute to the  $\text{He}^+$  ion loss (grad  $B$ ,  $E \times B$  and parallel). Calculated from the magnetic and electric fields given in Fig. 2. Suffixes r, p, and t indicate the radial, poloidal, and toroidal components, respectively.

Radial profiles of gradient  $B$  drift,  $E \times B$  drift, parallel drift caused by the misalignment of the beam (here,  $2.5^\circ$  misalignment is assumed), and summation speed of them are shown in Fig. 3. For  $\delta L = 10 \text{ cm}$ ,  $\tau_{\text{loss}} = \delta L/v_d$  is typically 3 -  $10 \mu\text{s}$  in the assumed profiles. Loss of  $\text{He}^+$  ions from the detection region is determined mainly by the gradient  $B$  and  $E \times B$  drift motions in the outer region, and by the parallel drift motion in the core region.

For the given magnetic configuration and electric field, the toroidal components of the gradient  $B$  and  $E \times B$  drift motions, which are the largest components of drift motion in the outer region, have the same direction unfortunately, since  $E_r$  is produced by the rapid loss of electrons, and gradient  $B$  and  $E_r$  have opposite directions (negative

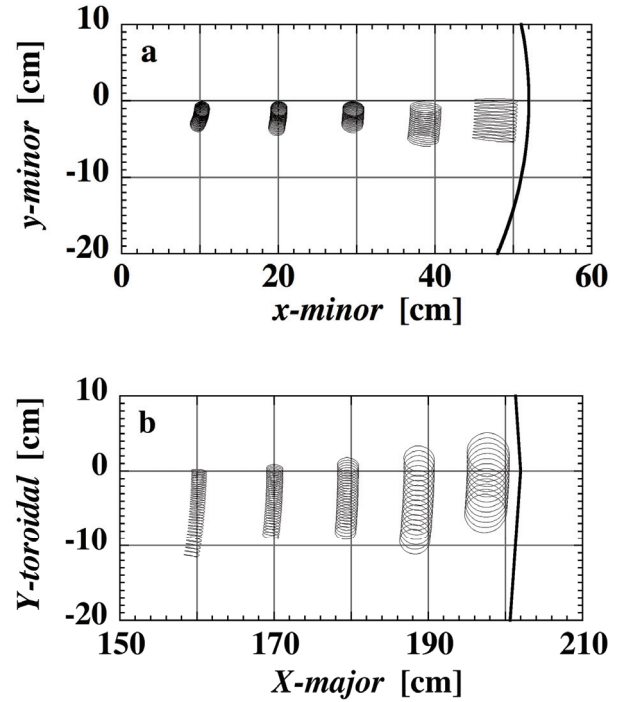


Fig. 4 Orbits of  $\text{He}^+$  ions ionized at several points along the He beam. Side view of orbits in a poloidal cross-section (a) and view from the top of the torus (b).

gradient  $B$  and positive  $E_r$ ).

Examples of orbits of  $\text{He}^+$  ions until  $10 \mu\text{s}$  from the ionization at various positions along the beam, are shown in Fig. 4. In the calculation, a magnetic nearly identical with that given in Fig. 2 is used, but the effect of electric field is not considered. Correction of toroidal effect in the MST is also taken into account. The estimation is close to a realistic situation, although the toroidal effect is not significant in RFP, since the poloidal field has the same amplitude as the toroidal field and the curvature of the magnetic field line is mainly determined by the minor radius. As can be seen in Fig. 4, the  $\text{He}^+$  ions stay in the detection region for more than  $5 \mu\text{s}$ . When the electric field is taken into account, the total drift velocity near the edge approximately doubles and the loss time is reduced to  $3 \mu\text{s}$ .

By solving equations (7) and (8) numerically, the radial variations of  $n_{\text{HeG}}$  and  $n_{\text{HeM}}$  are obtained, and are shown in Fig. 5 for the case of  $\gamma_{\text{meta}} = 0.1$ . For the assumed temperature and density profiles, only 12.5% of the initial beam can penetrate into the center of the plasma.  $I_{4686}$  calculated from Eq. (6) is also shown in Fig. 5, and is greater than  $10^{14}$  photon/s in the region of  $0.3 < r/a < 0.9$ .

The number of photons counted by the detector may be given by

$$N_{\text{count}} = I_{4686} \gamma_D \tau_{\text{detect}} (d\Omega/4\pi), \quad (10)$$

where  $\gamma_D$  is the total sensitivity of the detection system,  $\tau_{\text{detect}}$  is the accumulation time of the measurement, and  $d\Omega$  is the solid angle of the detector. By using plausible

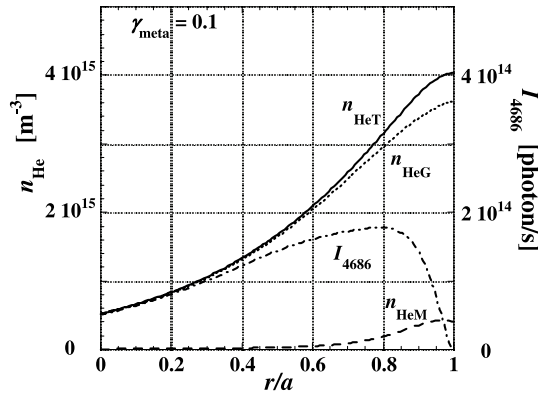


Fig. 5 Radial profiles of penetration of the He beam and intensity ( $I_{4686}$ ) of  $\text{He}^+$  line radiation (468.6 nm) at the detection region. In the case with initial metastable state ratio of 0.1 ( $\gamma_{\text{meta}} = 0.1$ ). Densities of ground state ( $n_{\text{HeG}}$ ), metastable state ( $n_{\text{HeM}}$ ), and sum of them ( $n_{\text{HeT}}$ ) are also shown.

values, we are able to estimate the detected photon count. Here we assume values of  $\gamma_{\text{D}}$ ,  $\tau_{\text{detect}}$ , and the radius of the detection window ( $r_{\text{D}}$ ) as  $10^{-3}$ , 10 ms, and 0.025 m, respectively. The distance to the detection window ( $L_{\text{D}}$ ) from the radiation region is assumed to be two times of the minor radius ( $a$ ).  $d\Omega = \pi r_{\text{D}}^2 / 4a^2$  is  $2 \times 10^{-3}$  for  $a = 0.5$  m and  $N_{\text{count}}$  is greater than  $1.6 \times 10^5$  for  $0.3 < r/a < 0.9$ . This  $N_{\text{count}}$  will probably be sufficient for spectroscopic measurement.

If it is possible to use a smaller value of radiation intensity, the time resolution can be improved by using a shorter  $\tau_{\text{detect}}$  or the  $I_{\text{b0}}$  can be reduced to the 10 mA range. These results indicate that the proposed magnetic field measurement method is feasible in typical RFP plasma similar to MST, if a He neutral beam with  $I_{\text{b0}} \sim 10 - 100$  mA,  $E_{\text{b}} \sim 1$  keV, and  $r_{\text{b}} \sim 1.5$  cm is realized and  $E_{\text{rw}}$  remains less than 5 kV/m.

The photon count near the central region can be increased by increasing the beam energy, since the magnetic field strength near the center is larger than that near the edge region. The field is  $2.7 B_{\text{pa}}$ , as shown in Fig. 2, at the center, and the gyroradius is smaller than 2.5 cm even for  $E_{\text{b}} = 4$  keV. By increasing the beam energy, the beam can penetrate deeper, and a high current beam is expected. Combination of these two effects enable  $I_{4686}$  greater than  $10^{14}$  photon/s in the central region with  $E_{\text{b}} = 4$  keV and  $I_{\text{b0}} = 250$  mA.

## 4. Discussion

### 4.1 Estimation of Doppler width

The maximum value of Doppler width of the 468.6 nm line with beam energy of  $E_{\text{b}}$  is given by  $\Delta\lambda_{\text{M}} [\text{nm}] = 0.68 (E_{\text{b}} [\text{keV}])^{0.5}$ . The observed maximum value is  $\Delta\lambda_{\text{Max}} = \Delta\lambda_{\text{M}} \sin \phi$  where  $\phi$  is the angle between the rotational axis of gyromotion and the straight line drawn from the center of gyromotion to the detection position when the gy-

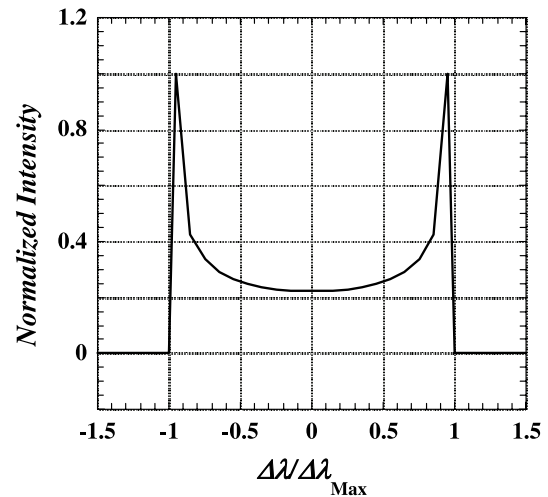


Fig. 6 Profile of Doppler broadening due to gyromotion with a monochromatic energy. Wavelength and intensity are normalized by their maximum values. Wavelength is divided into 20 sections.

roradius is much smaller than the distance to the detection position.

The broadening profile is expected to be quite different from the Gaussian profile, since the Doppler broadening is caused by the gyromotion of  $\text{He}^+$  ions with a monochromatic energy ( $E_{\text{b}}$ ). The expected time variation of Doppler shift of a single  $\text{He}^+$  ion is given by  $\Delta\lambda_{\text{D}} = \Delta\lambda_{\text{Max}} \cos(\omega_{\text{c}}t + \Omega_0)$  during the gyromotion, where  $\omega_{\text{c}}$  is the gyrofrequency,  $t$  is time, and  $\Omega_0$  is the initial phase.

In the Doppler broadening measurement, it is common to divide a certain wavelength region into  $N$  separate parts with a discrete step of  $\Delta\lambda_{\text{s}}$ . Setting  $\Delta\lambda_{\text{s}} = \Delta\lambda_{\text{Max}}/N$ , the duration time  $\delta t$  within which  $\Delta\lambda_{\text{D}}$  stays between  $\lambda$  and  $\lambda + \Delta\lambda_{\text{s}}$  can be estimated. It is reasonable to assume that the line radiation has an equal probability around the orbit of gyromotion, and thus, the statistical intensity of the line radiation between  $\lambda$  and  $\lambda + \Delta\lambda_{\text{s}}$  is proportional to the  $\delta t$ . Figure 6 shows an example of the expected broadening profile with  $N = 20$  and the vertical value normalized by its maximum at the largest shift.

As shown in Fig. 6, the profile of Doppler broadening is quite different from the Gaussian profile in the usual temperature measurement. A sharp increase and decrease appear around the maximum shift position, which makes it easy to determine the maximum Doppler width necessary in the present measurement. In actual situations, several mechanisms causing other broadenings of the line radiation are present, and the shape of the profile is not so sharp as shown in Fig. 6. These additional broadenings determine the limitation of the accuracy of the measurement.

The radial variation of the direction of the magnetic field line is more than  $90^\circ$  between the center and edge of RFP plasma, since the direction of toroidal magnetic field at the edge is reversed with respect to that at the center.

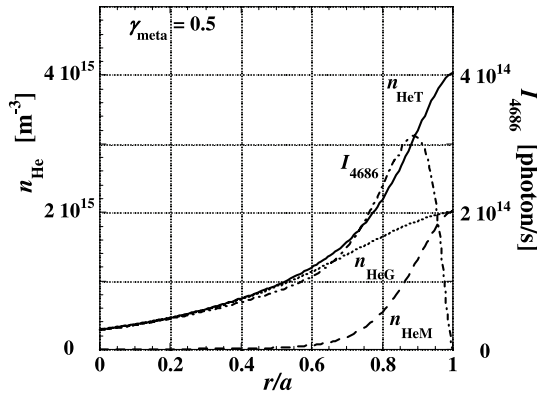


Fig. 7 Same graphs as show in Fig. 5, but for the case with a different initial metastable state ratio ( $\gamma_{\text{meta}} = 0.5$ ).

Similarly, it is several tens of degrees in a spherical tokamak (ST). Therefore, resolution in the order of  $10^\circ$  will be sufficient to measure the radial variation of the direction of the magnetic field. However,  $E_b$  must be low in those machines, since the magnitude of  $r_L$  should satisfy a required spatial resolution in weak magnetic fields (as low as 0.3 T).

For example, the beam with a low  $E_b$  of 1 keV gives  $r_L = 3$  cm and  $\Delta\lambda_M = 0.68$  for  $B = 0.3$  T. Then the required resolution becomes less than 0.068 nm. It is not difficult to obtain this resolution by the ordinary Doppler broadening measurement method, and is larger than that of the fine line structure and Zeeman effect of the 468.6 nm line.

In typical tokamaks, which have a major radius of 1.5 m, minor radius of 0.5 m,  $B = 3$  T and  $q = 3$ , the beam with  $E_b = 10$  keV gives  $r_L = 1$  cm and  $\Delta\lambda_M = 2.2$  nm. However, the maximum radial variation of the angle of the magnetic field line is about  $10^\circ$  between the center and the edge, even though the non-circular and toroidal effects are taken into account, since the toroidal magnetic field is much larger than the poloidal one. This means that a resolution of the order of  $1^\circ$  is required to obtain reasonable spatial resolution. Consequently, very high resolution in the Doppler width measurement, of the order of  $\sim 0.02$  nm, is required, which will not be impossible but is difficult, and the limitations by other causes of line broadening, such as the fine line structure, Zeeman effect, and motional Stark effect should be taken into account.

## 4.2 Effect of the metastable state

As described before, the effect of the metastable state of the He neutral atoms can be critical for penetration of the beam. If the value of  $\gamma_{\text{meta}}$  is high at the injection point, the penetration length is reduced considerably. An example is shown in Fig. 7, where a He beam with  $\gamma_{\text{meta}} = 0.5$  is examined. The ionization of He atoms is localized near the boundary, and hence, the beam intensity is reduced by a factor of about two at the center.  $I_{4686}$  is also reduced by a factor of about two.

The  $I_{4686}$  profiles with several  $\gamma_{\text{meta}}$  values are shown

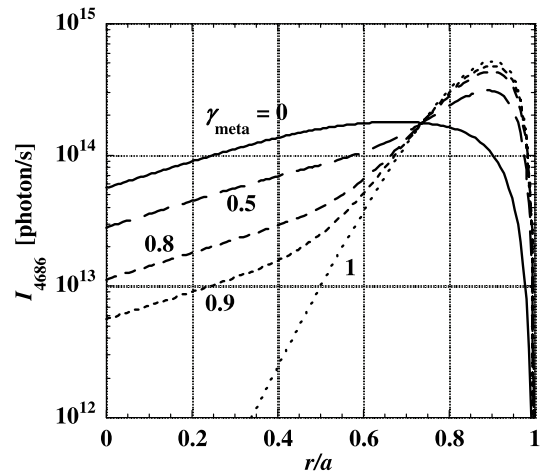


Fig. 8 Radial profiles of intensity of line radiation ( $I_{4686}$ ) with different initial metastable state ratios ( $\gamma_{\text{meta}}$ ).

in Fig. 8. It is shown that, except for the  $\gamma_{\text{meta}} = 1$  case, the central value of  $I_{4686}$  is nearly proportional to the value of  $\gamma_{\text{meta}}$ . For the  $\gamma_{\text{meta}} = 0.9$  case, the intensity of  $I_{4686}$  is reduced by an order of magnitude. However,  $I_{4686}$  is  $6 \times 10^{12}$  photon/s even in this case, and the Doppler measurement is probably possible.

The 468.6 nm line becomes very strong near the boundary region for large  $\gamma_{\text{meta}}$ . If information near the boundary is required, e.g., the radial profile of the magnetic field direction near the reversal surface, then a He beam with large  $\gamma_{\text{meta}}$  is preferred. We will be able to select a proper  $\gamma_{\text{meta}}$  according to the position for which information is required, if we can control  $\gamma_{\text{meta}}$ , although the way to control it is not yet known.

## 4.3 Rough estimation of parameters in a tokamak

For a typical medium sized tokamak, as considered in the Sec. 4.1 ( $B = 3$  T,  $R/a = 1.5$  m / 0.5 m,  $T = 1$  keV, and  $n = 5 \times 10^{19}$  m $^{-3}$ ), if we use the same values of  $\gamma_D$ ,  $\tau_{\text{detect}}$ , and  $r_D$  as before ( $10^{-3}$ , 10 ms, and 0.025 m), and also assume that the distance to the detector is  $\sim 3a = 1.5$  m ( $d\Omega = 9 \times 10^{-4}$ ) because of the plasma elongation, we can examine the feasibility of this measurement. The value of  $r_L$  is 1 cm for  $E_b \sim 10$  keV, which can provide a good spatial resolution. The estimated value of  $I_{4686}$  is greater than  $2 \times 10^{14}$  photon/s and  $N_{\text{count}}$  may be greater than  $1.5 \times 10^5$  counts for  $I_{b0} = 1$  A. These values will also be sufficient for the spectroscopic measurement. Here we use a large value of  $I_{b0}$  ( $=1$  A), which is not difficult to achieve for the high beam energy region ( $E_b = 10$  keV) using the present beam technology. Considering the estimated intensity of radiation,  $I_{b0}$  can be reduced to about 0.1 A.

Since the magnetic field is strong in tokamaks, and the gyroradius is not too large for the measurement even with the relatively high  $E_b$ , a heavy atomic species with

high ionization potential, such as neon can be used. It should be noted, however, that, as estimated in Sec. 4.1, very high resolution in the wavelength is required and the fine line structure, Zeeman effect and motional Stark effect in the line radiation should be carefully considered, since the beam velocity (hence  $\Delta\lambda_M$ ) is reduced for the heavy atom.

#### 4.4 Other aspects

A He neutral beam that can penetrate into hot plasma with a reasonable density value can be used for other diagnostic applications. For example, the plasma electron density profile can be estimated by observing the decay of the line emission from the neutral beam atoms. Fluctuation of electron density can also be estimated by observing the fluctuation of the He or He<sup>+</sup> line emission, although care is required in the analysis, since the He and He<sup>+</sup> ion densities are dependent on the integral effect of the plasma density and temperature along the beam path, through which the He beam has penetrated to the detection position. Another possible application is to measure the trace of the drift motion of He<sup>+</sup> ions in a wide spatial region by monitoring the line emission, which can be used to estimate the electric field strength and direction if the profile of the magnetic field is known. If the beam is injected with a significant velocity component parallel to the magnetic field, then the magnetic field line can be traced by observing the line emission from He<sup>+</sup> ions.

### 5. Conclusion

The feasibility of measuring the radial variation of the direction of the magnetic field using He neutral beam injection is studied at high temperature, medium density plasma. The injected He neutral beam is ionized by collision with plasma electrons, and the ionized beam He<sup>+</sup> ions rotate around the magnetic field line (gyromotion). By measuring the Doppler broadening of the line radiation from these He<sup>+</sup> ions (e.g., 468.6 nm) during the gyromotion, the direction of the magnetic field can be determined.

By estimating the penetration of the He beam into the plasma and the radiation intensity of the 468.6 nm line, it is examined whether the radial variation of the magnetic field line direction can be determined in the reversed field pinch plasma, which is similar to the MST ( $R/a = 1.5 \text{ m} / 0.5 \text{ m}$ ,  $B_{pa} = 0.3 \text{ T}$ ). Considering realistic profiles of the temperature, density, and magnetic and electric fields, and including the effect of He beam atoms in the metastable state, the radial variations of the densities of He beam in the ground state, and in the metastable state are calculated separately. Excitation from the ground state to the metastable state and ionization from these two states are taken into account.

The number of He<sup>+</sup> ions in the detection region is calculated from the balance between the production and loss of He<sup>+</sup> ions. The production is the ionization of He beam atoms in the detection region, and the loss is caused by the

ionization of He<sup>+</sup> to He<sup>2+</sup> and the drift motion of He<sup>+</sup> ions from the detection region. The drift motions are calculated for a real magnetic field similar to that in the MST. From radial profiles of the number of He<sup>+</sup> ions and the plasma density, the radial variation of intensity of the 468.6 nm line radiation can be obtained.

The results show that a He beam having  $E_b = 1 \text{ keV}$  and  $I_{b0} = 100 \text{ mA}$  (possibly  $\sim 10 \text{ mA}$ ) is sufficient to obtain a radiation intensity that can measure the angle of the magnetic field lines with reasonable spatial ( $\sim 6 \text{ cm}$ ) and time ( $\sim 10 \text{ ms}$ ) resolutions. The estimated radiation intensity,  $I_{4686}$ , is greater than  $10^{14}$  photon/s for  $0.3 < r/a < 0.9$ .

By using a He beam with  $E_b = 10 \text{ keV}$  and  $I_{b0} = 1 \text{ A}$  (possibly  $\sim 0.1 \text{ A}$ ), which is not difficult with the present beam technology, this diagnostic technique can be used in tokamaks having a magnetic field of  $B = 3 \text{ T}$ ,  $R/a = 1.5 \text{ m} / 0.5 \text{ m}$ , temperature =  $1 \text{ keV}$  and density  $5 \times 10^{19} \text{ m}^{-3}$ , although very high wavelength resolution is required for Doppler measurement.

### Acknowledgement

The authors are grateful to Prof. Takako Kato of Chubu University and Dr. Motoshi Goto at National Institute of Fusion Science, Japan, for their valuable and important advice on the cross-sections and rate coefficients of ionization and excitation for He atoms and ions. This study was financially supported by the Budget for Nuclear Research of the Ministry of Education, Culture, Sports, Science and Technology, based on the screening and counseling of the Atomic Energy Commission.

- [1] S.P. Hirshman, D.K. Lee, F.M. Levinton *et al.*, *Phys. Plasmas* **1**, 2277 (1994).
- [2] D.J. Den Hartog, D. Craig, D.A. Ennis *et al.*, *Rev. Sci. Instrum.* **77**, 10F122-1 (2006).
- [3] P.E. Young, *Rev. Sci. Instrum.* **56**, 896 (1985).
- [4] D.L. Brower, Y. Jiang, W.X. Ding and S.D. Terry, *Rev. Sci. Instrum.* **72**, 1077 (2001).
- [5] I.D. Kaganovich, E.A. Startsev and R.C. Davidson, *Phys. Plasmas* **11**, 1229 (2004).
- [6] H. Tawara and A. Russek, *Rev. Modern Phys.* **45**, 178 (1973).
- [7] T. Kato and R.K. Janev, *Nucl. Fusion Special Suppl.* **3**, 33 (1992).
- [8] A.A. Korotkov and R.K. Janev, *Phys. Plasmas* **3**, 1512 (1996).
- [9] Y. Yagi, Y. Maejima, Y. Hirano *et al.*, *Nucl. Fusion* **43**, 1787 (2003).
- [10] R. Bartiromo, V. Antoni, T. Bolzonella *et al.*, *Phys. Plasmas* **6**, 130 (1999).
- [11] S.C. Prager, J. Adney, A. Almagri *et al.*, *Nucl. Fusion* **45**, 276 (2005).
- [12] G.S. Voronov, *Atomic Data and Nuclear Data Tables* **65**, 1 (1997).
- [13] K. Rinn, F. Melchert and E. Salzborn, *J. Phys. B* **18**, 3783 (1985).
- [14] K.M. Aggarwal, K.A. Berrington, A.E. Kingston and A. Pathak, *J. Phys. B* **24**, 1757 (1991).
- [15] W.L. Wiese, M.W. Smith and B.M. Glennon, "Atomic

- Transition Probabilities” **1**, 6-7 (1966), National Standard Reference Data Series, NBS USA, NSRDS-NBS 4.
- [16] H.B. Gilbody, Nucl. Fusion Special Suppl. **3**, 55 (1992).
- [17] G.F. Abdrashitov, V.I. Davydenko, P.P. Deichuli *et al.*, Rev. Sci. Instrum. **72**, 594 (2001).
- [18] H. Sakakita, S. Kiyama, Y. Hirano *et al.*, Jpn. J. Appl. Phys. **45**, 8531 (2006).